Available online at www.sciencedirect.com
SCIENCE DIRECT®
International Journal of Heat and Mass Transfer 48 (2005) 4695–4703
International Journal of HEAT and MASS TRANSFER
www.elsevier.com/locate/ijhmt

# Numerical investigation of the new regenerator–recuperator scheme of VOC oxidizer

K.V. Dobrego [a,*], N.N. Gnesdilov [a], I.M. Kozlov [a], V.I. Bubnovich [b], H.A. Gonzalez [c]

[a] *Heat and Mass Transfer Institute, Chemical Physics Laboratory, National Academy of Sciences of Belarus, P. Brovki Street 15, Minsk 220072, Belarus*
[b] *Department of Mechanical Engineering, University Santiago de Chile, B.O'Higgins 3363, Casilla 10233, Santiago, Chile*
[c] *Department of Mechanical Engineering, Universidad Politécnica de Cataluña Av. Diagonal 647, 08028 Barcelona, Spain*

Received 10 June 2005
Available online 31 August 2005

**Abstract**

The new regenerator–recuperator scheme of filtration combustion VOC oxidizing reactor is under research. Its main characteristics, such as maximum temperature of reactor, temperature of exhaust gases, NO emission and others are calculated and compared with the same characteristics of other types of reactors (co-flow filtration combustion wave reactor, counter-flow heat exchange recuperative reactor, reverse flow regenerative reactor). It is shown that the regenerator–recuperator scheme provides important advantages (wide range of flow rate, and equivalence ratio of the combustible, low temperature of the exhaust gases) compared to conventional schemes.


*Keywords:* Filtration combustion (FC); Heat recuperation; Heat regeneration; Porous media; Volatile organic components (VOC); Oxidizer

## 1. Introduction

Recreation of polluted flue gases remains an actual problem for a variety of mechanical, chemical and biochemical technologies [1,2]. There are numerous industrial methods to recreate flue gases: sorption, condensation, combustion (conventional or catalytic), membrane separation, chemical/biochemical transformation of pollutants to neutral components [1,2]. The sorption process of gas purification consumes sorbents which have limited lifetime and demand recreation or replacement. Condensation to liquid phase is appropriate only to components characterized by relatively high temperature of condensation and in the case of high concentration of pollutants [1]. Direct combustion of the polluted air in open flames is not effective economically if the process is not combined with an industrial boiler, furnace or power generator. Membrane separation, catalytic oxidizing, chemical or biochemical transformation of the pollutants are rather selective and, in addition, expensive. Therefore they may be efficient only for specific cases [1,2].

* Corresponding author. Tel.: +375 17 2842217; fax: +375 17 2842212.
*E-mail address:* kdob@itmo.by (K.V. Dobrego).

0017-9310/$ - see front matter © 2005 Elsevier Ltd. All rights reserved.
doi:10.1016/j.ijheatmasstransfer.2005.07.003

**Nomenclature**

| | |
|---|---|
| $C_{p,i}$ | heat capacity of $i$th gas component, J/K/mol |
| $\overline{C}_p$ | average molar heat capacity of gas, J/K/mol |
| $\mathbf{D}$ | gas diffusivity tensor |
| $\mathbf{D}_\mathrm{d}$ | dispersion diffusivity tensor |
| $D_p$ | longitudinal component of dispersion diffusivity |
| $D_\mathrm{t}$ | transverse component of dispersion diffusivity |
| $D$ | diffusivity coefficient, $\mathrm{cm}^2/\mathrm{s}$ |
| $d_0$ | bedding particle diameter, m |
| $d_1$ | diameter of the internal tube, m |
| $d_2$ | diameter of the external tube, m |
| $G$ | gas flow rate, $\mathrm{m}^3/\mathrm{h}$ |
| $H_i$ | molar enthalpy of $i$th component, J/mol |
| $h_i$ | mass enthalpy of $i$th component, J/kg |
| $\mathbf{I}$ | unit matrix |
| $k_0$, $k_1$ | filtration permeabilities |
| $L$ | burner length, m |
| $M$ | average molecular weight of gas, kg/mol |
| $m$ | porosity |
| $Pr$ | Prandtl number |
| $p$ | pressure, Pa |
| $p_0$ | outlet pressure, Pa |
| $R$ | absolute gas constant |
| $\mathbf{s}_i$ | diffusion flux of $i$th chemical component, $\mathbf{s}_i = \rho_\mathrm{g}\mathbf{D}\nabla Y_i$ |
| $\mathbf{q}$ | heat flux in gas phase, $\mathbf{q} = \mathbf{\Lambda}\nabla T_\mathrm{g}$ |
| $T$ | temperature, K |
| $T_0$ | initial temperature of the system, K |
| $T_\mathrm{ad}$ | adiabatic temperature of combustion, K, $\Delta T_\mathrm{ad} = T_\mathrm{ad} - T_0$ |
| $\mathbf{u}$ | gas filtration velocity vector, m/s |
| $U_\mathrm{G}$ | superficial gas velocity, m/s |
| $X_i$ | molar fraction |
| $x$ | transverse coordinate, m |
| $Y_i$ | mass fraction of the $i$th gas chemical component |
| $z$ | longitudinal coordinate, m |
| $z_\mathrm{f}$ | front position |
| $z_\mathrm{r}$ | front position for flow reverse (switch), m |

*Greek symbols*

| | |
|---|---|
| $\alpha_\mathrm{vol}$ | heat exchange coefficient, $\mathrm{W/K/m}^3$ |
| $\varepsilon$ | emissivity of the bedding particles |
| $\varphi$ | equivalence ratio |
| $\eta_\mathrm{c}$ | dimensionless temperature, have sense of effectiveness |
| $\mathbf{\Lambda}$ | heat conductivity tensor $\mathbf{\Lambda} = c_p\rho_\mathrm{g}\mathbf{D}$ |
| $\lambda$ | conductivity, W/m/K |
| $\mu$ | gas viscosity, Pa s |
| $\rho$ | density, $\mathrm{kg/m}^3$ |
| $\dot{\rho}_i$ | mass generation of $i$th component due chemical reactions |
| $\sigma$ | Stefan–Boltzmann constant |
| $\tau_z$, $\tau_r$ | axial and radial components of the velocity vector projection |

*Subscripts*

| | |
|---|---|
| 1 | relates to internal tube or fuel |
| 2 | relates to external tube or oxidant |
| g | gas |
| s | solid |

The widely spread air pollutants—volatile organic components (VOC)—phenol, formaldehyde, acetone, benzole and others—have considerable heat content and may be eliminated by oxidation in inert porous media or filtration combustion [3–6]. Filtration combustion provides effective heat recirculation and consequently low energy costs of the process. Even in the case of low concentration of VOC (~1 mass%) the combustion process may be self-sustained due to the heat content of the pollutants. Takeno and Sato [9] researched sustained combustion of methane–air mixture in steady-state recuperative reactor with equivalence ratio as low as $\Phi = 0.026$.

Physical aspects of the filtration combustion (FC) in inert porous media are discussed in [4,7,8] and other papers. One of the principal features of FC is internal heat recirculation in the combustion wave, due to heat exchange between gas and solid in the preheat zone of the combustion wave. Practical systems designed for combustion of low calorific fuels utilize external heat recirculation in addition to internal. These heat recuperation is realized by means of counter-flow heat exchange between incoming and exhaust gases and heat regeneration due to periodical reverse of flow direction (Fig. 1). The first mentioned scheme works in steady state regime, the second works in non-steady periodical regime. Both schemes are examined in laboratory installations [3,4,9–11] and utilized in industrial VOC oxidizers produced by Thermatrix [12], ReEco-Stroem [13] and other companies.

The main technical difficulties of the regenerative scheme of reactor are connected with the need to sustain reliable operation of the mechanical switcher valves, particularly in conditions of increased temperature of the gas [3–5,10]. The disadvantage of the steady recuperative scheme of the reactor is the relatively narrow range of the gas mixture flow rate when heat recuperation efficiency is high.

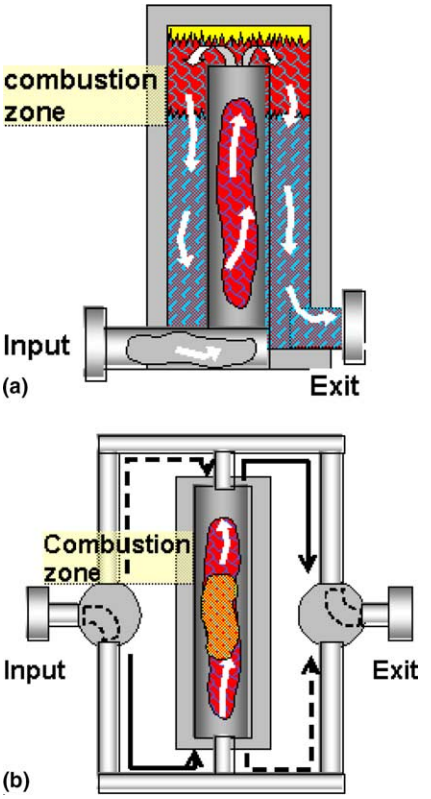


Fig. 1. Schemes of external heat recuperation. (a) Heat recuperation by means of counter-flow heat exchange, (b) heat regeneration due to periodical reverse of flow direction.

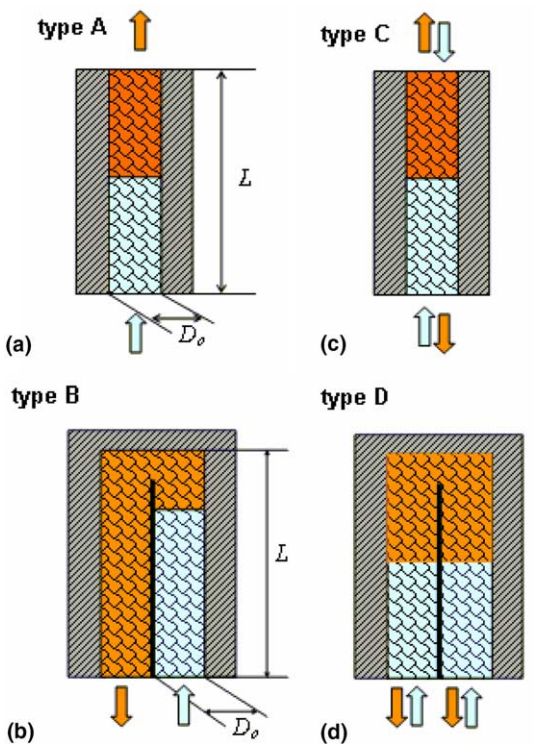


Fig. 2. Schemes of filtration combustion VOC oxidation reactors. (a) Co-flow propagating FC wave (moving bed) reactor, (b) counter-flow heat exchange recuperative reactor, (c) reverse flow regenerative reactor, (d) regenerative–recuperative reactor.

This article presents results of numerical simulations for four different schemes of VOC oxidizers (Fig. 2), and provide comparison between the results of simulations. The regenerative–recuperative burner is based on a conventional recuperative scheme burner (Fig. 1(a)) added with a system of periodical gas flow reversing. This arrangement makes both mechanisms of external heat recirculation work synergistically and compensates to a large extend disadvantages of both regenerative and recuperative schemes: makes it possible to obtain high efficiency of heat recirculation for a wide range of flow rates, decreases temperature of the exit gas and hence softens the operating conditions for switch valves.

We simulated four types of VOC oxidation processes using filtration combustion in inert porous media: combustion in propagating FC wave (Fig. 2(a)), combustion in a recuperator FC system (Figs. 1(a) and 2(b)), regenerator FC system (Figs. 1(b) and 2(c)) and combustion in a new type regenerative–recuperative system (Fig. 2(d)). For idealized model reactors (two-dimensional plain geometry, adiabatic walls, one step brutto chemical kinetics) the temperature, filtration, concentration and pressure fields were calculated for different gas flow rates and heat content. The NO generation by Zeldovich's mechanism was calculated for different combustion regimes. The comparison of the mentioned reactor schemes with regards to the principal characteristics of the VOC oxidation process was performed. Based on the simulation results the considerable advantages of the regenerative–recuperative scheme of VOC oxidizer can be concluded.

## 2. Problem statement

A regenerative–recuperative (RR) burner scheme may be realized by combining a conventional recuperative scheme (Figs. 1(a) and 2(b)) with a system of automated gas flow reversing (Figs. 1(b) and 2(c)). An idealized scheme of this type of reactor is presented in Fig. 2(d). For quantitative characterization of the RR scheme we compared four types of model reactors: quasi-stationary propagating FC wave (or moving bed) reactor (Fig. 2(a)), stationary recuperative reactor with counter-flow heat exchange between incoming and outgoing gas (Fig. 2(b)), reverse flow regenerative reactor

Table 1
Heat content of methane–air mixture at different $\Phi$

| $\Phi$ | $X_{CH_4}$ (%) | $\Delta H$ (J/kg) | $\Delta T_{ad}$ (K) |
|---|---|---|---|
| 1 | 0.095 | 2.760E+06 | 2026 |
| 0.8 | 0.0775 | 2.232E+06 | 1715 |
| 0.6 | 0.0597 | 1.693E+06 | 1370 |
| 0.4 | 0.04031 | 1.142E+06 | 981 |
| 0.3 | 0.03054 | 8.612E+05 | 766 |
| 0.2 | 0.02057 | 5.774E+05 | 533.8 |
| 0.1 | 0.01039 | 2.904E+05 | 278.8 |
| 0.05 | 0.00522 | 1.456E+05 | 142.1 |

(Fig. 2(c)), new RR reactor (Fig. 2(d)). Note that the moving bed reactor scheme is not used for VOC oxidizing due to technical complexity, although it should be considered as a possible scheme.

We considered 2-D plane geometry adiabatic reactors. Practical oxidizers may be supplied with perfect insulation and correspond well to adiabatic idealization. To compare operation parameters of the reactors geometrical similarity was conserved: length of the reactor chamber ($L$) and channel width ($D_0$) was the same for reactors A, B, C and D. Air polluted with VOC was modeled by lean methane–air mixture. Methane molar fraction $X_{CH_4}$, specific heat of the reaction and adiabatic temperature growth are determined by equivalence ratio $\Phi$, defined as fuel/air ratio normalized by stoichiometric ratio $\Phi = \frac{F/A}{(F/A)_{stoich}}$, see Table 1. We suppose air contain $N_2 = 79\%$, $O_2 = 21\%$ mole fraction.

For simulation of the cyclic regimes of the oxidizers of types C and D the criteria of the flow reverse should be established. Here we used the following algorithm. First, the front position along the reactor was determined as a coordinate of the point at the center line of the reactor chamber where the temperature was $T^* = \frac{T_{s,max}+T_{s,min}}{2}$. Here $T_{s,max}$ and $T_{s,min}$ represent the maximum and minimum temperature along the above mentioned line. The filtration flow was reversed when the front reached coordinate $z_r = 0.55 \cdot L$. For the case $\Phi = 0.05$ the combustion wave front position was determined as a point, where 85% of maximal heat release was reached and $z_r = 0.8 \cdot L$. (Optimization of the cyclic regime is an independent task which is not considered in this paper.)

## 3. Governing equations and algorithms

A typical set of equations for gas filtration combustion problem was used [17,18]: continuity equation for a gas mixture, filtration equation for the gas mixture, equation of mass conservation for each gas component, thermal conductivity equation for gas, thermal conductivity equation for porous media

$$\frac{\partial \rho_g}{\partial t} + \nabla(\rho_g \mathbf{u}) = 0, \tag{1}$$

$$-\nabla p = \frac{\mu}{k_0}\mathbf{u} + \frac{\rho_g}{k_1}|\mathbf{u}|\mathbf{u}, \tag{2}$$

$$\rho_g \cdot \partial Y_i/\partial t + \rho_g \mathbf{u} \nabla Y_i - \nabla \mathbf{s}_i = \dot{\rho}_i, \tag{3}$$

$$\rho_g c_p \partial T_g/\partial t + c_p \rho_g \mathbf{u} \nabla T_g - \nabla \mathbf{q} = \frac{\alpha_{vol}}{m}(T_s - T_g) - \sum_i (h_i \dot{\rho}_i + \mathbf{s}_i \nabla h_i), \tag{4}$$

$$(1-m)\rho_s c_s \frac{\partial T_s}{\partial t} - \nabla(\lambda \nabla T_s) = \alpha_{vol}(T_g - T_s). \tag{5}$$

Eqs. (1)–(5) are added with the equation of state for the gas mixture $\rho_g = \frac{pM}{RT_g}$. Average molar mass $M$ is determined via component concentration $1/M = \sum_i Y_i/M_i$. Here $\dot{\rho}_i$ is mass density variation of $i$th component due to chemical reactions, $\mathbf{s}_i = \rho_g \mathbf{D} \nabla Y_i$ is a diffusion flux of $i$th chemical component, $\mathbf{D} = D_g \mathbf{I} + \mathbf{D}_d$, where $\mathbf{D}_d$ is a tensor of dispersion diffusion, depending on gas average-mass velocity $\mathbf{u}$ and is expressed through longitudinal $D_p$ and transverse $D_t$ components as follows:

$$\mathbf{D}_d = \begin{bmatrix} D_p\tau_z^2 + D_t\tau_r^2 & (D_p - D_t)\tau_z\tau_r \\ (D_p - D_t)\tau_z\tau_r & D_p\tau_r^2 + D_t\tau_z^2 \end{bmatrix}, \quad \boldsymbol{\tau} = \frac{\mathbf{u}}{|\mathbf{u}|}. \tag{6}$$

$\mathbf{q} = \boldsymbol{\Lambda} \nabla T_g$ heat flux in gas phase. $\boldsymbol{\Lambda}$ is a tensor of thermal conductivity. It is determined similarly to the diffusion tensor, regarding disperse mixing of gas, $\boldsymbol{\Lambda} = c_p \rho_g \mathbf{D}$. Other definitions are introduced in the nomenclature list.

We used the following definitions of the parameters. Coefficient of volumetric heat transfer is [7,17]

$$\alpha_{vol} = \frac{\lambda_g 6(1-m)}{d_0^2}\left[2 + 1.1 Pr^{1/3}\left(\frac{\rho_g u_g d_0}{\mu}\right)^{0.6}\right]. \tag{7}$$

Thermal conductivity includes conductivity $\lambda_s$ and radiation component

$$\lambda = \lambda_s + \frac{32\sigma d_0 m \varepsilon}{9(1-m)} T_s^3. \tag{8}$$

Molar heat capacity of $k$th substance $C_{p_k}$ and average molar heat capacity $\overline{C}_p$, $k$th component molar enthalpy $H_k$ are expressed via polynomials as recommended in CHEMKIN packages [19]. Average mixture enthalpy per 1 mol of mixture $\overline{H}$ is calculated via component enthalpy and molar concentrations.

Permeability in filtration equation (2) is defined as follows:

$$k_0 = \frac{d_0^2 m^3}{A(1-m)^2}, \quad k_1 = \frac{d_0 m^3}{B(1-m)}. \tag{9}$$

Here Ergun's constants $A$ and $B$ are specified for particular porous medium (for polished balls bedding $A = 150$, $B = 1.75$).

Molecular diffusion coefficient, coefficient of viscosity and heat conductivity of gas mixture are approximated with corresponding nitrogen properties,

$$D_g = 0.18\left(\frac{T}{273}\right)^{1.75}\frac{p_0}{p}\ \mathrm{cm^2/s},\quad p_0 = 1.013\ \times\ 10^5\ \mathrm{Pa},$$
$$\lambda_g = 1.4\ \times\ 10^{-2} + 4.8\ \times\ 10^{-5}\cdot T,\ \mathrm{W/m/K},$$
$$\mu = 4.4\times 10^{-7}\cdot T^{0.65}\ \mathrm{Pa\,s}. \tag{10}$$

Formulas (10) have characteristic accuracy of ~5% at $T = [300\text{–}2500]$ K.

We considered one step combustion reaction $CH_4 + O_2 \xrightarrow{k} CO_2 + H_2O$, with the reaction rate $k = 2.17\times 10^8 \exp(-15{,}640/T_g)$, $\frac{m^3}{s\,mol}$ for the first order by $CH_4$ and $O_2$ kinetics. To estimate NO generation we used Zeldovich's thermal mechanism [14–16]

$$O + N_2 \overset{k,k_r}{\leftrightarrow} NO + N \tag{11}$$

where $k = 1.8\times 10^6 \exp(-38{,}370/T_g)$, $k_r = k/k_{eq}$, $k_{eq}$ is the equilibrium constant.

$$N + O_2 \overset{k,k_r}{\leftrightarrow} NO + O \tag{12}$$

where $k = 9.0\times 10^3 T \exp(-3273/T_g)$, $k_r = k/k_{eq}$, $k_{eq}$ is the equilibrium constant.

$$O_2 \overset{k,k_r}{\leftrightarrow} 2O \tag{13}$$

where $k = 1.82\times 10^{12} T^{-1} \exp(-59{,}380/T_g)$, $k_r = k/k_{eq}$, $k_{eq}$ is the equilibrium constant.

Initial gas temperature and temperature of the input gas is equal to $T_0 = 300$ K. Ignition of the system is simulated by preheating part of the porous carcass to high temperature.

Table 2
Standard case values

| | Dimension | Value |
|---|---|---|
| $d_0$ | m | $4.8\times 10^{-3}$ |
| $\lambda_s$ | W/m/K | 1.87 |
| $\Phi$ | mol/mol | 0.1 |
| $T_0$ | K | 300 |
| $U_G = u_g\cdot m$ | m/s | 1 |
| $L$[a] | m | 0.4, 0.8 |
| $D_0$ | m | 0.02 |
| $\varepsilon$ | dimensionless | 0.45 |
| $\alpha$ | $W/m^3/K$ | ~100,000 |
| $m$ | dimensionless | 0.4 |
| $\rho_s$ | $kg/m^3$ | 3987 |
| $c_s$ | J/kg/K | 1300.0 |
| $p_0$ | Pa | $1.01325\times 10^{-5}$ |

[a] For reactors of types B and D standard case is 0.4 m, and for type C standard L two times bigger.

Adiabatic boundary conditions and walls impermeability were used as boundary conditions for the problem

$$(\mathbf{n}\cdot\nabla)T_g = 0, \tag{14}$$
$$(\mathbf{n}\cdot\nabla)p = 0, \tag{15}$$
$$(\mathbf{n}\cdot\nabla)Y_i = 0. \tag{16}$$

The problem was solved by using Filtburn software package [17,18]. Eq. (3) is solved by iteration method or Newton's method with dumping. Then equation set (1) and (2) are iterated. Equation for pressure is solved by congradient method [20].

The values of the parameters for the standard case calculations are presented in Table 2. Simulations were carried out at standard case parameters if other is not defined.

## 4. Results and discussion

### 4.1. Maximum temperature of the porous carcass

The maximum temperature of the porous media $T_s$ was calculated for all types of reactors and different equivalence ratios ($\Phi = 0.05$, 0.1, 0.2 and 0.3) as a function of the gas superficial velocity $U_G = u_g\cdot m$. The same temperature data are presented in the dimensionless form $\eta_c = \frac{T_{s,max}-T_0}{\Delta T_{ad}}$ on the same graphs. It is easy to see that the lower heat content (adiabatic combustion temperature) of the mixture the higher dimensionless temperature is reached (Fig. 3) which is connected with heat recirculation efficiency.

Fig. 3 shows that operating regimes of reactors of type B and D are the same for the lower filtration rates. For the higher filtration rates, when a stationary operation regime is impossible, B-type reactor can not operate and D-type reactor switches to regime of cyclic flow reversing. The critical filtration rate when cycling starts depend on reactor design/geometry and on the criterion of flow reversing. The area of stationary operation widens for the higher calorific mixtures (higher $\Phi$).

Simulations show that among four types of reactors, A-type reactor provides maximum temperature Fig. 3(b). Practical application A-type reactor (moving FC wave) for VOC oxidizing encounters numerous difficulties. Each cycle of combustion should be started with ignition—preheating of the system, which leads to additional energy consumption. Another problem is instability of co-flow propagating waves [21].

Comparison of the regenerative (type C) and regenerative–recuperative (type D) reactors show that the former provides higher temperature for small and average flow rates, although at high filtration rates the temperature in the D-type reactor exceeds one in the regenerative reactor (type C), see Fig. 3.

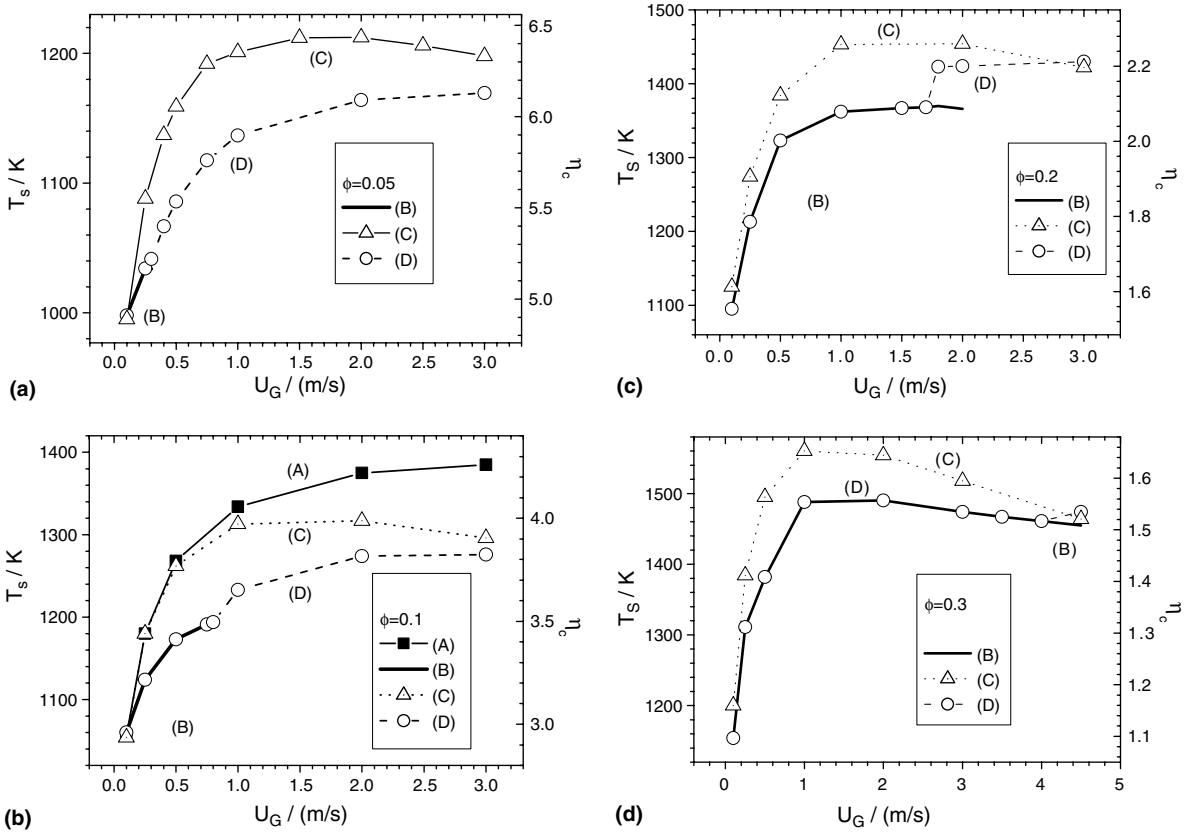


Fig. 3. Maximum cycle temperature of the porous carcass and dimensionless temperature $\eta_c$ as a function of the gas filtration velocity. (a) $\Phi = 0.05$, (b) $\Phi = 0.1$, (c) $\Phi = 0.2$, (d) $\Phi = 0.3$. Other parameters are from Table 2. Three types of the reactors—B, C and D are considered.

### 4.2. Temperature of exhausted gases

The temperature of the gas at the exit of the reactor is an important parameter, characterizing the operating conditions and effectiveness of the oxidizer. Under stationary operation regime exit gas temperature is defined by adiabatic combustion temperature of the gas and quality of thermal insulation of the reactor. Output gas temperature influences the choice of technical equipment and service of reactor: additional heat exchangers, radiators at pipelines etc. may be necessary. In the case of reverse flow reactors, it is important to sustain relatively low temperature of switch-valves for their reliable and long-term operation.

The values of the maximum-in-cycle mass averaged temperatures at the exit of reactors C and D are presented in Fig. 4. It follows from the data that exit gas temperature in the new regnerative–recuperative reactor is much lower than in the regenerative reactor. This result is explained by additional heat exchange between incoming and outgoing gas flow. Quantitatively the difference in output temperature implies hundreds of Kelvin, which is a very significant advance for reliable operation of the system of switch valves.

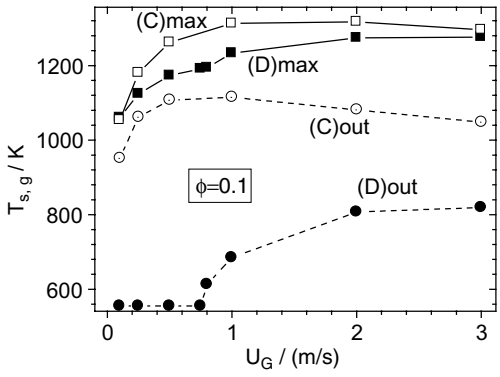


Fig. 4. Maximum cycle temperature of the carcass and of the exit gases for typical (Table 2) conditions of operation for C- and D-types of reactors, $\Phi = 0.1$.

### 4.3. Influence of total reactor length and flow reversing criterion

The difference in gas exit temperature between reactors of types C and D increases with the growth of the total length of the reactor (Fig. 5) and for optimized practical devices may reach the value of the order of 300–400 K.

Criterion of flow reversing defines not only critical flow rate, but also thermal characteristics of the reactor operation in cyclic regime. The maximum temperature of the porous carcass during the half-cycle is presented in Fig. 5, for reactor types C and D.

It follows from Fig. 5(a) that in the C-type reactor $T_{s,max}$ grows with the increase of reactor length $L$ (switch coordinate $z_r$ increases proportionally to $L$). This may be explained by lower heat losses.

Fig. 6 demonstrates maximum carcass temperature as a function of wave position $z_f$ for reactors of type C and D in the case of $z_r = 0.22$ m. The arrows show the time sequence of the points in the cycle.

Note that switch control coordinate $z_r$ cannot be too close to the total reactor length (in the case of C-type reactor), because relatively wide hot zone area is necessary for combustion reignition after the flow reverse. The graphs of Fig. 7(a) indicates that the maximum cycle temperature for $z_r = 0.72$ (Fig. 4) is lower than

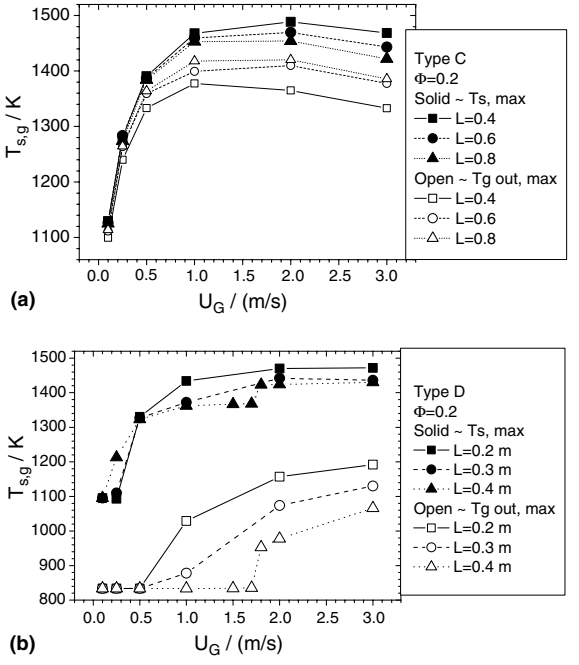


Fig. 5. Maximum cycle solid carcass temperature $T_{s,max}$ and maximum cycle mass mean exit gas temperature $T_{g,out,max}$. The reactor length as denoted in the legend. (a) Type C, (b) type D. Other parameters are from Table 2.

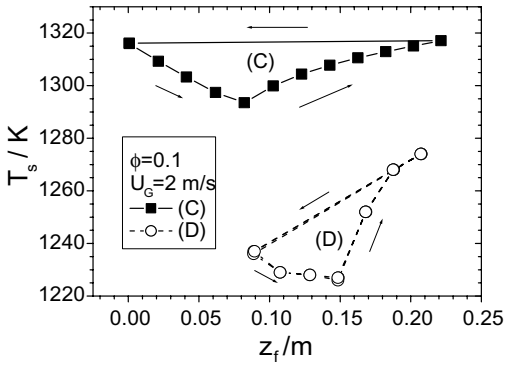


Fig. 6. Maximum carcass temperature during the half-cycle as a function of front position in the recuperative burner. Standard case geometry, methane concentration $\Phi = 0.1$, filtration velocity—as denoted on the picture. Other parameters are from Table 2. Arrows indicate time sequence of the points in cycle.

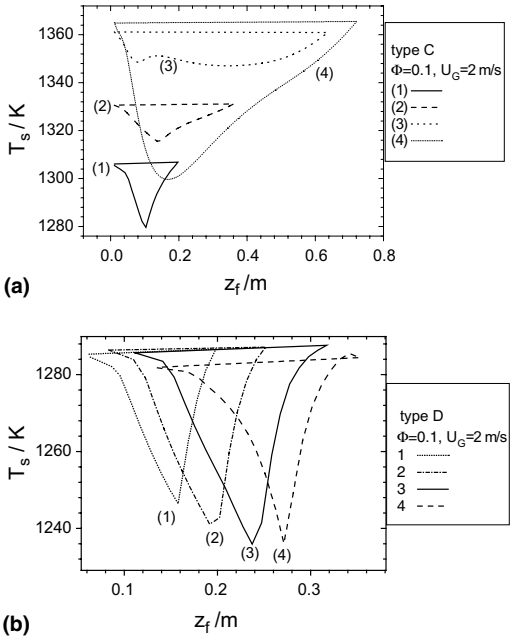


Fig. 7. Maximum temperature of the porous carcass during the half-cycle as a function of reverse control coordinate $z_r$. Reactors of C- and D-types are considered. (a) Reactor of C-type. (1) Stands for case where $z_r = 0.2$, (2) $z_r = 0.36$, (3) $z_r = 0.64$, (4) $z_r = 0.72$; (b) Reactor of D-type. (1) Stands for case where $z_r = 0.2$, (2) $z_r = 0.26$, (3) $z_r = 0.32$, (4) $z_r = 0.36$.

for $z_r = 0.36$ and $z_r = 0.64$ (graphs 2 and 3). For $z_r > 0.74$ combustion wave cannot reignite.

Some different dependence takes place in the D-type reactor where maximum carcass temperature does not

vary strongly with switch control coordinate $z_r$ (Fig. 7(b)).

### 4.4. NO formation

NO formation in FC system was simulated by using kinetic model (13)–(15). Calculations show very low level of NO concentration in exhausts for all types of reactors. The results obtained for the reactors of C- and D-types for $\Phi = 0.05$ are presented in Fig. 8. One can see that NO concentration is lower for D-type reactor at higher flow rates $U_G > 0.2$ m/s (reverse flow operation). In the stationary regime ($U_G < 0.2$ m/s) NO concentration is higher in the D-type reactor (Fig. 8), which is explained by higher temperature and residence time for gas particles. The decay of NO concentration observed in the C-type reactor at $U_G > 1.5$ m/s corresponds to the decrease of maximum temperature (see Fig. 3(b)). Fig. 9 demonstrates NO variation in time (one cycle) for the D-type reactor and $\Phi = 0.3$. The sharp peak in the center of the curve corresponds to a gas flow direction switch when a small portion of the gas passes the hot zone twice.

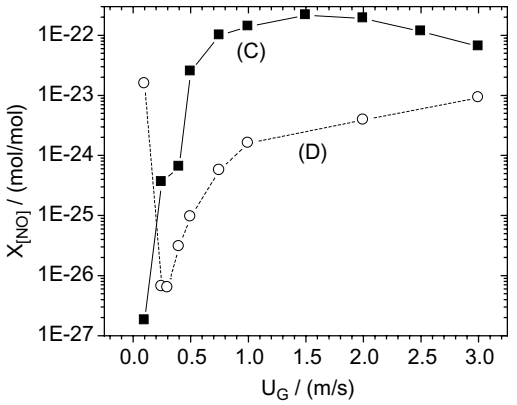


Fig. 8. NO concentration in exit gas as a function of gas velocity $U_G$. Reactors of C- and D-type, $\Phi = 0.05$.

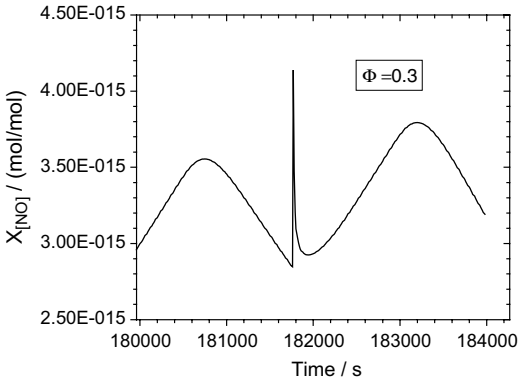


Fig. 9. Typical dependence of NO concentration in exit via time. D-type reactor, $\Phi = 0.3$, $U_G = 0.5$ m/s. Other parameters are from Table 2.

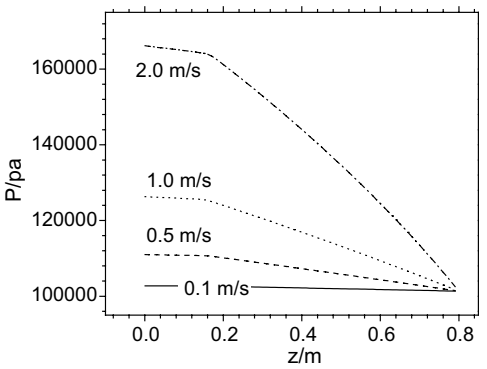


Fig. 10. Typical pressure dependence on the distance from inlet for different superficial velocities $U_G$. C-type reactor. Length of the system is 0.8 m. Other parameters are from Table 2.

### 4.5. Pressure drop

Pressure profiles for the C-type reactor at different superficial velocities are presented in Fig. 10. The graphs show that at filtration velocity 1.0 m/s the pressure gap is of the order of $0.25p_0$ for the given parameters of the reactor. The value of the pressure gap does not depend crucially on the type of reactor.

## 5. Conclusions

Numerical simulation of temperature characteristics and other operating parameters for model VOC oxidation reactors was performed. Four reactor schemes were taken into consideration: the first three are—quasi-steady filtration combustion wave, conventional recuperative and regenerative schemes; the fourth is a new scheme combining recuperative and regenerative types of reactor.

Comparative simulation of the mentioned reactor schemes demonstrated peculiarities of the thermal regimes of each of the reactors. Particularly, the highest temperature can be achieved in quasi-steady filtration combustion wave (Fig. 3(b)). Maximum temperature in the recuperative–regenerative reactor grows faster than in regenerative one and at certain flow rate exceeds the maximum temperature reachable in regenerative reactor (Fig. 3(c)).

Compared to recuperative scheme (heat exchange due to gas products counter-flow) the recuperative–regenerative scheme provides considerable (several times) expansion of the flow rate range and admissible VOC concentrations.

Simulations show that in the cyclic regime of operation recuperative–regenerative reactor generates less NO compared to the regenerative reactor (type C).

An important advantage of the recuperative–regenerative scheme is the relatively low temperature of the exit gases. The mass average maximum temperature at the exit may be 100–400 °C lower than in regenerative type of reactor, which leads to utilization of simpler and cheaper peripheral devices and more reliable operation of the switch valves.

Other technical parameters of the model VOC oxidizers such as pressure drop in the reactor and NO generation in the process were obtained. The data may be used for primary evaluation of the working parameters of practical VOC oxidizers. The performed simulations demonstrate good prospects for practical realization of the regenerative–recuperative scheme for VOC oxidizers and other similar processes.

## Acknowledgements

This work was supported by FONDECYT project 1050241, Academia Politecnica Aeronautica de Chile and Fund for Fundamental Research of Belarus project T05-259.

## References

[1] Selecting the most appropriate HAP emission control technology, The Air Pollut. Consultant 3 (2) (1993) 1.1–1.9.
[2] Yu.S. Matros, A.S. Noskov, V.A. Chumachenko, Catalytic Recreation of Industrial Flue Gases (in Russian), Nayka Publ., Novosibirsk, 1991, pp. 22–37.
[3] F. Contarin, A.V. Saveliev, A.A. Fridman, L.A. Kennedy, Int. J. Heat Mass Transfer 46 (2003) 949–961.
[4] L.A. Kennedy, A.A. Fridman, A.V. Saveliev, Superadiabatic combustion in porous media: wave propagation, instabilities, new type of chemical reactor, Int. J. Fluid Mech. Res. 22 (1995) 1–26.
[5] J.G. Hoffman, R. Echigo, H. Yoshida, S. Tada, Experimental study on combustion in a porous media with a reciprocating flow system, Combust. Flame 111 (1997) 32–46.
[6] W.D. Binder, R.J. Martin, The destruction of air toxic emissions by flameless thermal oxidation, Presented at 1993 Incineration Conference, Knoxville, Tennessee, 4 May 1993.
[7] K.V. Dobrego, S.I. Zhdanok, Physics of Filtration Combustion of Gases (in Russian), HMTI Publ., Minsk, 2002.
[8] K. Hanamura, R. Echigo, S. Zhdanok, Superadiabatic combustion in a porous medium, Int. J. Heat Mass Transfer 36 (13) (1993) 3201–3209.
[9] T. Takeno, K. Sato, An analytical study on excess enthalpy flames, Combust. Sci. Technol. 20 (1979) 73.
[10] M.K. Drayton, A.V. Saveliev, L.A. Kennedy, A.A Fridman, Y.E. Li, Superadiabatic partial oxidation of methane in reciprocal and counterflow porous burners, in: Proc. of the 27th Sympos. (Int.) on Combust, Pittsburg, PA, 1998, pp. 1361–1367.
[11] A.N. Migoun, A.P. Chernukho, S.A. Zhdanok, Numerical modeling of reverse-flow catalytic reactor for methane partial oxidation, in: Proc. of the Nonequilibrium processes and their applications. V Int. School-Seminar. Minsk, 2000, pp. 131–135.
[12] www.thermatrix.com.
[13] http://www.eco-web.com/.
[14] Ya.B. Zeldovich, G.I. Barenblatt, V.B. Librovich, G.M. Makhviladze, Mathematical Theory of Combustion and Explosion, Plenum, New York, 1985.
[15] J. Warnatz, U. Maas, R.W. Dibble, Combustion, Springer-Verlag, Berlin, Heidelberg, 1996.
[16] W.C. Gardiner Jr. (Ed.), Combustion Chemistry (in Russian), Springer-Verlag, M.:Ми, 1988.
[17] K.V. Dobrego, I.M. Kozlov, S.A. Zhdanok, N.N. Gnesdilov, Modeling of diffusion filtration combustion radiative burner, Int. J. Heat Mass Transfer 44 (2001) 3265–3272.
[18] K.V. Dobrego, I.M. Kozlov, N.N. Gnesdilov, V.V. Vasiliev, 2DBurner—software package for gas filtration combustion systems simulation and gas non-steady flames simulation, Heat and Mass Transfer Institute, Minsk, 2004, Preprint N1.
[19] R.J. Kee, F.M. Rupley, J.A. Miller, CHEMKIN-II: a fortran chemical kinetics package for the analysis of gas phase chemical kinetics, Sandia National Laboratory, SAND89- 8009B, 1989.
[20] R.W. Hockney, J.W. Eastwood, Computer Simulation Using Particles, McGraw-Hill Inc., 1981.
[21] K.V. Dobrego, V.A. Bubnovich, I.M. Kozlov, C.E. Rosas, Dynamic of filtration combustion front perturbation in the tubular porous media burner, Int. J. Heat Mass Transfer 46 (2003) 3279–3289.